FISKERTON, LINCOLNSHIRE

CORROSION RATES FOR MODERN EXPERIMENTAL IRON SAMPLES BURIED CLOSE TO THE IRON AGE CAUSEWAY

ARCHAEOLOGICAL CONSERVATION REPORT

VANESSA FELL

ARCHAEOLOGICAL SCIENCE

Fiskerton, Lincolnshire: Corrosion Rates for Modern Experimental Iron Samples Buried Close to the Iron Age Causeway

Vanessa Fell

Abstract

Samples of modern experimental iron were buried in the vicinity of the Iron Age causeway at Fiskerton in December 2003 as part of a joint project to assess the effects of rewatering on the Iron Age wooden causeway and artefacts. The samples were recovered at 6, 12, 18 and 30 month burial durations. Corrosion products were characterised by X-ray diffraction analysis and are reported on elsewhere. Corrosion rates for the iron samples are reported on here.

Key words

Burial environments
Conservation
Modern
Iron

Contents

Introduction

Experimental iron samples were buried at Fiskerton, Lincolnshire, as part of a joint project to assess the effects of rewatering on the Iron Age wooden causeway and artefacts (Last 2005). The experimental materials, comprising iron, copper, bone, antler and horn, were inserted in the ground in December 2003 for which the methods of burial and recovery are described elsewhere (Fell et al 2005). The iron samples are being studied by the present writer whereas the other materials are the responsibility of other researchers.

The iron samples were recovered at 6, 12 and 18 months burial durations with the final 30 month samples extracted in June 2006. Those recovered to 18 months were analysed by X-ray diffraction (XRD) to determine the chemical nature of the corrosion products (Fell 2005; Fell and Williams 2004). Initially, the corrosion products were retained *in situ* on the bars in case additional XRD analyses were required to check identifications of compounds. Therefore corrosion rates were not evaluated at that time, and this present report redresses that matter. Other results that will be presented in the future are those from the XRD analysis of the final 30 month burial durations as well as interpretations of all the results alongside the groundwater data.

Figure 1. Rods of iron samples as recovered after 30 months burial. The iron samples – bars of c. 50mm length – are tied on to the rods between the white spacers and are partly hidden in these images by soil that is in the recesses.
Left: Rod 4 of Cluster 2 shown leaning against the fencing surrounding the groundwater monitoring point. Centre: upper part of Rod 6 of Cluster 2 showing iron staining that occurred at around 0.5m below ground level. Right: upper part of Rod 4 of Cluster 1.

Corrosion rate is defined as the rate at which a corrosion reaction proceeds (Shrier et al 1994, 21:73). There are several methods that can be employed to determine corrosion rate but none is straight-forward to apply, or simple to calculate. Nor are there standard units of expression. The methods chosen will depend on purpose and convenience, and all methods depend on various assumptions. The methods and relevant calculations employed for the Fiskerton samples are explained in the next section and Appendix 1, the theory and methodology of which has relied mainly on Shrier et al (1994, 19.1), with other standard texts also providing information (eg Bardal 2004; Thompson 1971; Wranglén 1985).

The iron samples (or 'bars' or 'coupons') were buried at two locations, Cluster 1 near the north delph of the River Witham, and Cluster 2 at 25 metres away to the north. The locations are adjacent to the groundwater monitoring probes (see Williams 2005). Each installation rod comprised an inert support rod with eight samples of iron attached and separated by inert spacers (Figure 2). The lowest sample (coupon 1) was buried to 1.6 metres below ground level and the uppermost (coupon 8) was buried to 0.5 metres below ground level. For each burial duration, a rod of eight samples was recovered from both locations. The experiment was curtailed at 30 months, when the remaining three rods were recovered from both locations (Rods 4, 5 and 6). At the time of writing, Rods 5 and 6 have not yet been analysed; some samples are stored dry, others are stored wet.

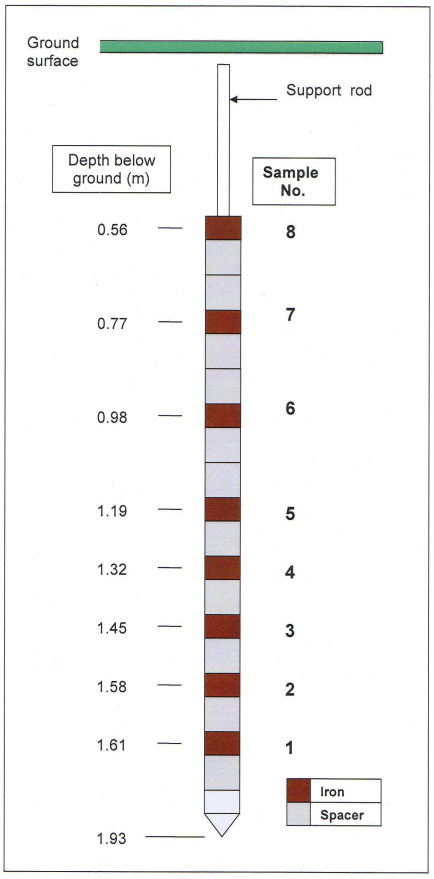

Figure 2. Diagram of an installation rod showing sequence and depths of iron coupons

Methods of expressing corrosion rate
There are three commonly used methods for calculating corrosion rate:

(i) *Mass (or weight) loss* rate, or weight loss per unit area per unit time – expressed as, for example, grams per square metre per day ($g.m^{-2}.d^{-1}$)

(ii) R*ate of penetration,* or average thickness reduction of the material per unit time – expressed as, for example, millimetres per year ($mm.y^{-1}$)

(iii) *Corrosion current density* – measured through attached electrodes, as amps per square metre ($A.m^{-2}$)

Methods (i) and (ii) above are based on measurements of loss of metal through corrosion, which is easier to determine than any increase in weight due to conversion to corrosion products. This is because the corrosion products will be of various species and with varying amounts of water depending on atmospheric humidity.

The *mass loss rate*, or the mass of metal turned into corrosion products per unit area of surface per unit of time, will depend on the area of metal exposed, as well as the duration of exposure. Surface area is calculated from dimensions. Duration of exposure is measured in any sensible unit, common in days (24 hour period) or years (365.25 days).

Mass loss units are commonly converted to depths of penetration to enable comparisons with other data. *Depth or rate of penetration* (ii, above), is the increase in corrosion depth per unit of time, and takes into account the density of the metal being corroded in order to convert surface area to a volume.

Corrosion rate is also expressed as c*orrosion current density (iii, above),* measured through attached electrodes and is therefore not applicable to the Fiskerton samples.

Errors
The principal assumptions that are made for any of these methods described above are firstly that the corrosion is uniform over the whole surface, and secondly, that corrosion occurred at a linear rate throughout the duration of the period of measurement. Non-uniform corrosion over a surface can be caused by factors such as geometry, surface condition, and electrolyte concentrations, which can result in localised corrosion such as pitting and crevice corrosion. Non-linear corrosion rates are caused by polarisation, passivation through the formation of protective surface layers, as well as changes in the environmental conditions.

In terms of the coupons under test, the ideal samples are thin circular discs so that edge effects are kept to a minimum and the surface area is large (Shrier et al 1994, 19:5). Surfaces should be free from mechanical cleaning effects such as polishing and should be degreased before use. For ease of calculation of surface areas, standard size coupons are preferable, and for statistical analysis, there should be five replicates. Additional errors can arise through the methods used to remove corrosion products during calculations to determine weight loss (see later).

Measuring mass loss

Mass loss is the difference in weight before and after exposure to the burial environment. Weight before exposure is readily measured but the value after exposure requires that the corrosion products are removed. This can be achieved through mechanical, electrolytic or chemical cleaning. Mechanical cleaning by air abrasion was tested on coupons for a similar previous study in woodland at Alice Holt, Hampshire, but the method was found to be time-consuming and not necessarily any better than chemical cleaning (Fell forthcoming). Electrolytic cleaning is the preferred method in industry (Shrier et al 1994, 19:119-121) but not available to us for the Fiskerton samples.

A chemical cleaning method was devised for the Fiskerton coupons and the agent selected was ethylenediamine tetra-acetic acid disodium salt ($EDTA.Na_2$) because this is a chelating agent and thus less likely to etch the metal surface. Because of the possibility of solid metal dissolving during this period, one set of eight coupons was resubmitted to a second period of four hours immersion in fresh solution and then reweighed.

Calculations

Methods to calculate both *mass loss* and *penetration rate* are given in Appendix 1, together with conversion methods since it is normal to cite both methods to enable comparisons. For the Fiskerton samples, corrosion rate is measured as mass loss expressed as grams per square metre per day ($g.m^{-2}.d^{-1}$), and as penetration rate expressed as millimetres per year ($mm.y^{-1}$) or sometimes more conveniently as µm per year, the basic equations for which are given below:

$$\text{Mass loss rate} = \frac{W}{A} \times \frac{1}{T} \quad (g.m^{-2}.d^{-1})$$

$$\text{Penetration rate} = \frac{W}{A} \times \frac{1}{T} \times 365.25 \times \frac{1}{\rho} \times 10^{-3} \quad (mm.y^{-1})$$

Where: W = mass loss in grams
A = surface area in square metres
T = time in days
ρ = density of iron

The metal coupons were measured and weighed before burial and then after recovery and removal of corrosion products. The approximate surface area of each coupon was calculated from the three main dimensions, ignoring the punched identification markings on each coupon. The volume of metal loss is the difference in weights before and after exposure to the burial environment, divided by density of the metal. The density (**ρ)** of the uncorroded ferritic metallic iron (99.9% Fe) is 7.87 $g.cm^{-3}$ or 7.87 x 10^3 $kg.m^{-3}$ (Brandes 1983, table 14.11). The relevant burial durations for the Fiskerton coupons are shown in Table 1.

Table 1. Burial durations for the Fiskerton experimental iron samples

Nominal duration	Burial duration	Real duration		
		Days	Weeks & days	Years
6 month	22 Dec 2003 – 22 June 2004	183	26 wks	0.5010
12 month	22 Dec 2003 – 08 Dec 2004	351	50 wks 1 day	0.9610
18 month	22 Dec 2003 – 22 June 2005	547	78 wks 1 day	1.4986
30 month	22 Dec 2003 – 25 June 2006	915	130 wks 4 days	2.5051

Methods

The metal coupons were measured and weighed before burial. After each recovery from site, the coupons were photographed (eg Figures 5 and 6) and were initially sampled for corrosion products in order that these could be characterised by XRD analysis (Fell 2005).

The coupons were then stripped of corrosion products in order that the weight of metal after burial could be calculated. The coupons were cleaned coarsely by scalpel (and the corrosion products retained) and then immersed in a 5% aqueous solution of EDTA.Na_2 with occasional brushing until the corrosion products had been removed. The surfaces of the coupons remained a dull grey colour presumed to be due to loss of the smoothed layer of surface grains. For the coupons buried for up to 18 months, periods of immersion of between one and four hours in a 5% aqueous solution were found to be adequate. The coupons buried for 30 months required rather longer and were left overnight for 21 hours for the Cluster 1 coupons, and 24 hours for Cluster 2 coupons (Figures 5 and 6). Coupons were rinsed in water, then alcohol, and dried at c. 80℃ or overnight with desiccant and then weighed to two decimal places.

Error trials were made on a set of coupons to test if the solution was causing any dissolution of the metal itself, rather than just the corrosion products. Eight coupons, serving as blanks (coupons 1 to 8 of 12 months Cluster 2 Rod 1), were immersed for a second period of 4 hours in EDTA.Na_2 solution. There was no weight variation except in one case of 0.01g loss (Appendix 2, a, coupon 8). The conclusion was that the EDTA.Na_2 solution did not have any significant effect on the dissolution of the metallic iron, and error calculations were thus avoided. In addition, all coupons from the 30 month burial duration series were immersed for additional 24 hour periods during which time the weights did reduce slightly (Appendix 2, b and c). The second sets of weights were thus applied for the calculations. (The weight losses seem more likely to be due to dissolution of intragranular iron corrosion products rather than dissolution of the metal.)

The corrosion rates were calculated from the equations shown earlier and detailed in Appendix 1,

Results

The dimensions and weights of the iron coupons prior to burial are given in Appendix 3 from which the surface areas of the coupons were calculated (Appendix 4). Corrosion rate calculations for coupons buried at Cluster 1 are given in Appendix 5, and those for Cluster 2 are given in Appendix 6. For convenience, the chemical names and formulae for the corrosion products detected previously are shown in Table 2.

Photographs of selected coupons are shown for Cluster 1 in Figure 3 (6 months), Figure 4 (18 months) and Figure 5 (30 months). Coupons for Cluster 2 are shown in Figure 6 (6 months) and Figure 7 (30 months). Note that the sets of coupons buried for different period are from different installation rods and thus they are not quite the same shapes and sizes, although all are approximately 50mm in length. The photographs of the stripped coupons compared with their parent coupons in Figures 5 and 7 are exceptions to this, being identical coupons although with some orientated at 180°. Note also that at 6 months bur ial duration, it was Rod 2 (not Rod 1) that was recovered from Cluster 2.

The data are best expressed graphically, as two-dimensional stacked column charts, three-dimensional column charts, and as line graphs. Mass loss rates are shown in Figure 8, and penetration rates are shown with a similar suite of charts in Figure 9.

Table 2. Corrosion products and other minerals detected by XRD

Mineral name	Formula	Common name
Goethite	α-FeOOH	Iron oxyhydroxide
Magnetite	Fe_3O_4	Iron oxide
Maghemite	γ-Fe_2O_3	Iron oxide
Siderite	$FeCO_3$	Iron carbonate
Lepidocrocite	γ-FeOOH	Iron oxyhydroxide
Akaganéite	β-FeOOH	Iron oxyhydroxide
Greigite	Fe_3S_4	Iron sulphide
Mackinawite	$Fe_{1+x}S$	Iron sulphide
Pyrite	FeS_2	Iron sulphide
Vivianite	$Fe_3(PO_4)_2.8H_2O$	Iron phosphate
Iron sulphide	FeS	Iron sulphide
Calcite	$CaCO_3$	Calcium carbonate
Quartz	SiO_2	Silicon dioxide

The corrosion effects on the samples recovered at 6 months show that those attached at the centre of the installation rods are more corroded than those at either end (eg Figure 3). These differences become more pronounced over time (eg Figure 4), until at 30 months, severe corrosion has occurred (Figures 5 and 7).

Figure 3. Iron samples from Cluster 1, Rod 1, after 6 months' burial showing coupons 1–8 in sequence, with coupon 1 at the left. Note that the coupons at either end are less corroded than those in the centre. Coupon lengths, c.50mm.

Figure 4. Iron samples from Cluster 1, Rod 3, after 18 months' burial showing coupons 1–8 in sequence, with coupon 1 at the left. Coupons 1 and 2 show typical orange-red accretions over black deposits, whereas coupon 3 reveals a lustrous layer of relatively thin corrosion products. Coupons 4 to 7 show both orange and black corrosion products. Coupon 8 (right) has some bare metal (visible at the top) plus a thin layer of orange and brown corrosion products.

At Cluster 1, it will be seen from Figures 3 and 4, and the charts in Figures 8 and 9, that the uppermost coupons 6–8 are little corroded. This may be because the upper soil at that location is well drained due to its proximity to the delph, and also because of the height difference between the ground surface and the water surface. Coupons 4 and 5, however, are severely corroded despite these normally lying below the water table. At the time of writing in 2006, the water levels at Cluster 1 have become raised to an average depth of 0.9m from the soil surface

compared with previous levels before rewatering in autumn 2004 of between 1.0m and 1.5m depth (J Williams pers comm). However, there can be fluctuations that are not recorded during the monthly water level measurements. This depth of 0.9m equates approximately to the position of coupon 6. Coupons 1–3 are also fairly corroded and again these lie below the normal water table. The rates of corrosion for the earlier recoveries are relatively consistent within their burial duration groups but the rates for coupons 1–5 have vastly increased over the final 12 months of burial, whereas the rates for coupons 6–8 have stabilised.

Figure 5. Iron samples from Cluster 1, Rod 4, after 30 months' burial. The upper photograph shows coupons 1–8 (left to right) as recovered and after removal from the installation rod. The lower image shows the same coupons after chemical stripping.

At Cluster 2, the water levels are now around 0.3m to 0.6m depth from the surface and are more consistent than the previous levels before rewatering in 2004 which ranged from 0.7m to 1.6m depth (J Williams pers comm). This means that all the coupons should lie below the water table for all or most of the time. Again, coupons 7 and 8 are consistent within their groups and are less corroded than the others at this location. Coupon 5 is the most corroded, and coupons 1–4 and 6 are also rather corroded although not as much as those from Cluster 1. The corrosion rates for all Cluster 2 coupons have also much increased during the final 12 months, although not as much as for Cluster 1.

Figure 6. Comparison of coupons 2, 4, 6 and 8 (left to right) from Cluster 2, Rod 2, after 6 months' burial. Coupons 2 and 4 exhibit thin dark corrosion products indicative of reduced species, whereas coupons 6 and 8 reveal orange and brown corrosion products indicative of oxidised species.

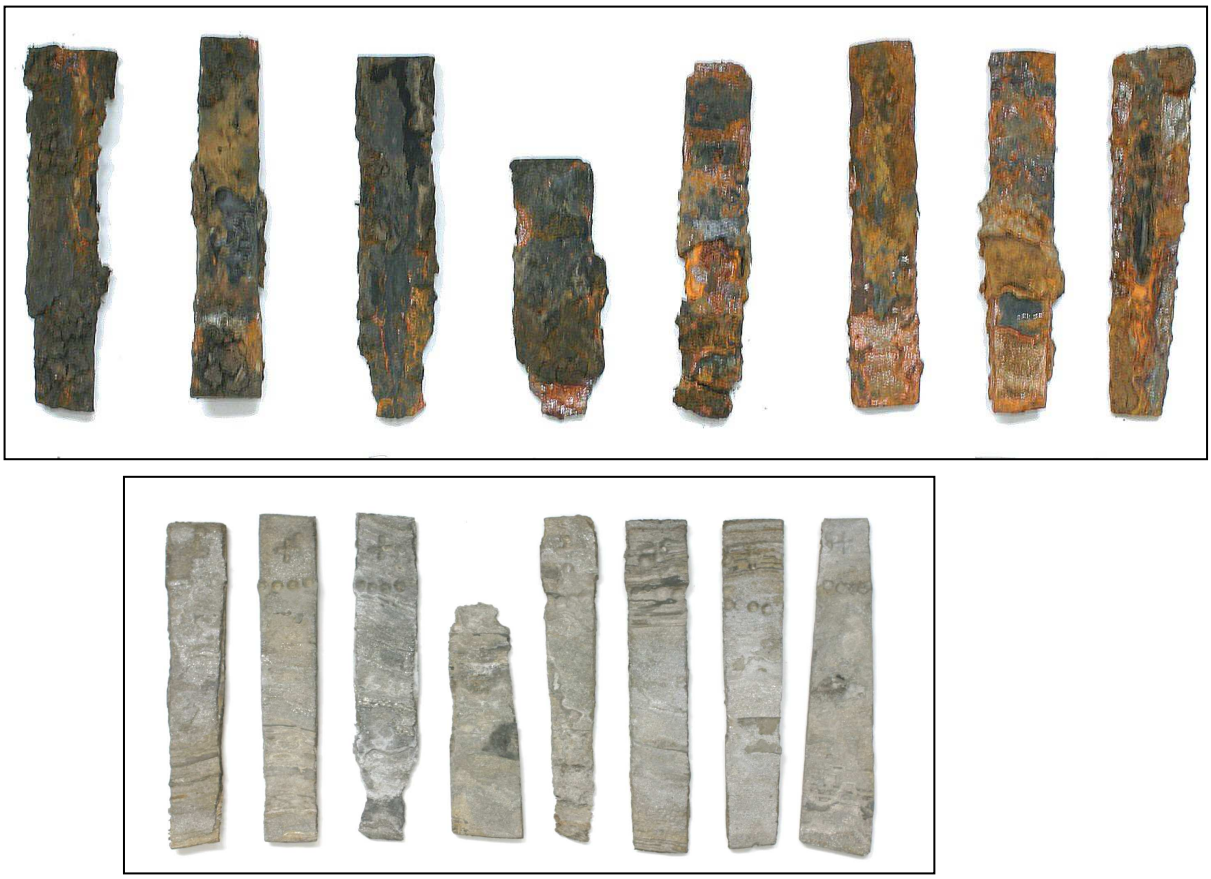

Figure 7. Iron samples from Cluster 2, Rod 4, samples after 30 months' burial. The upper photograph shows coupons 1–8 (left to right) as recovered and after removal from the installation rod. The lower image shows the same coupons after chemical stripping.

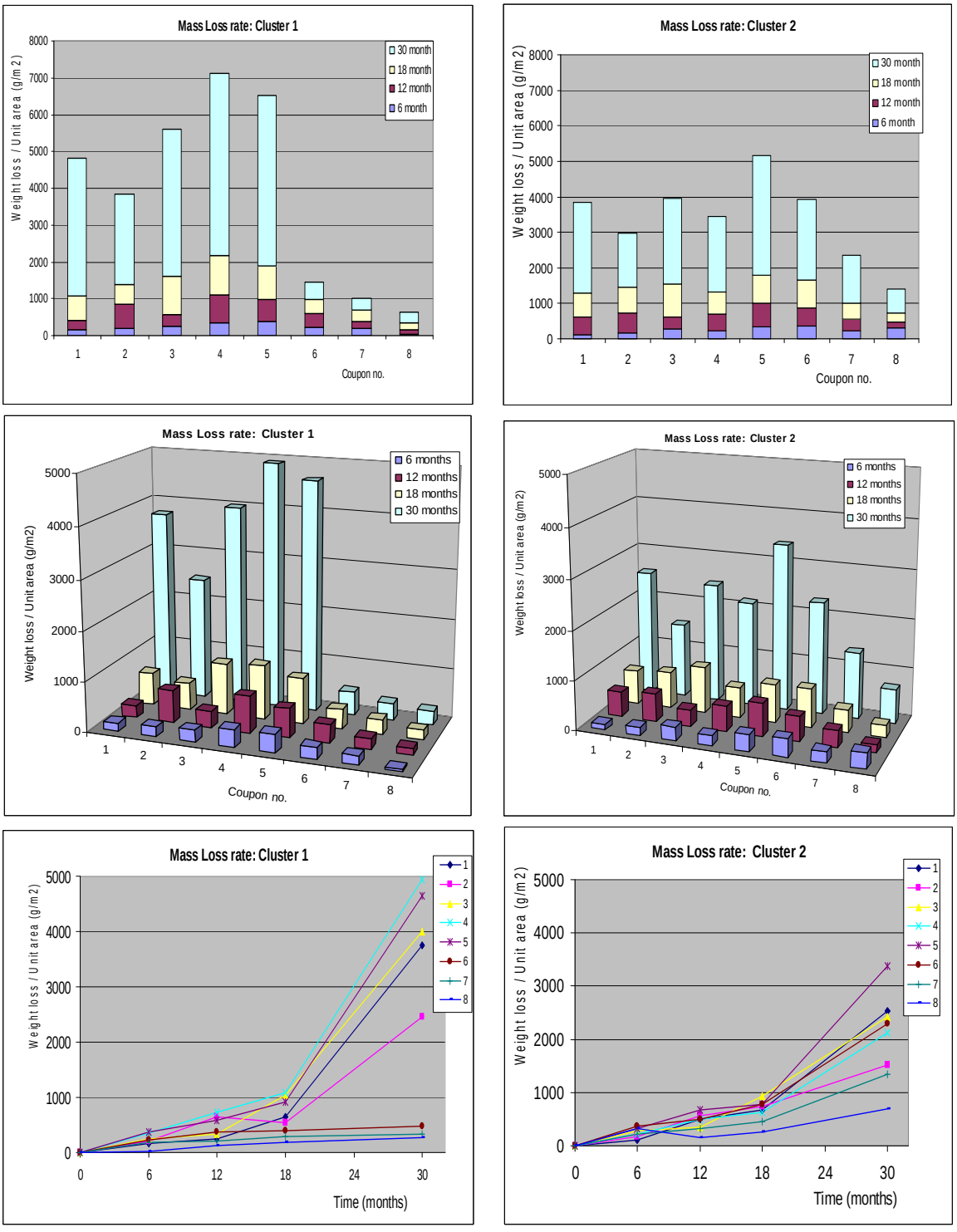

*Figure 8. Corrosion rates expressed as **Mass Loss Rates** for samples from Cluster 1 (left) and Cluster 2 (right). The data for the charts for each cluster are the same, but expressed in different ways. The upper two rows compare weight loss per unit area for each coupon at the four recovery periods of 6, 12, 18 and 30 months, showing that corrosion rates are non-linear and unexpectedly high, except for the uppermost coupons. The lowest pair of line graphs compare corrosion rate over time for each individual coupon showing that only the upper 3 coupons of Cluster 1 were relatively linear in corrosion rate.*

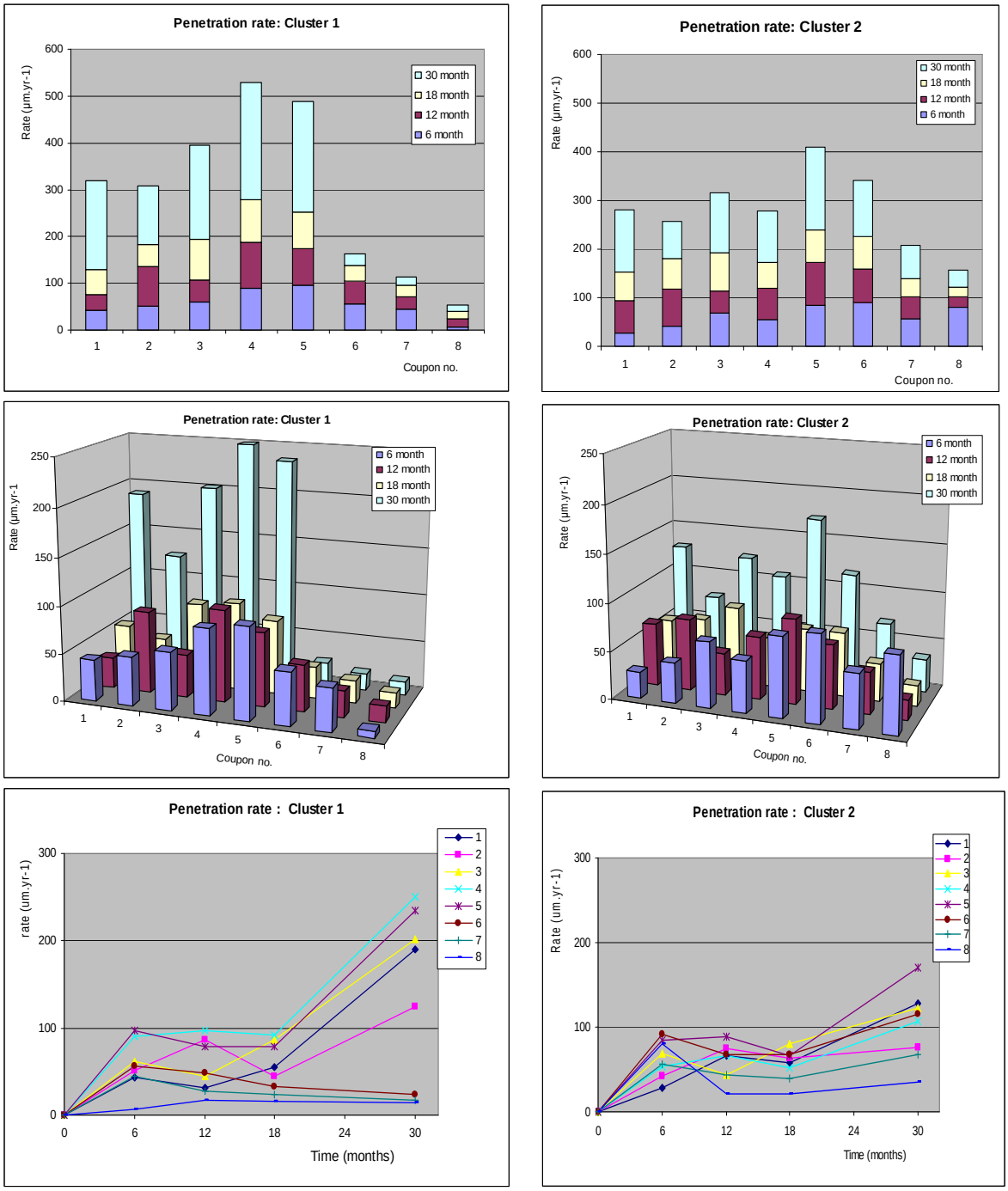

*Figure 9. Corrosion rates expressed as **Penetration Rates** for samples from Cluster 1 (left) and Cluster 2 (right). The data for the three charts for each cluster are the same, but expressed in different ways. The upper two rows compare penetration for each coupon at the four recovery periods of 6, 12, 18 and 30 months, showing that corrosion rates are non-linear and unexpectedly high, except for the uppermost coupons. The lowest pair of line graphs compare penetration rate over time for each individual coupon showing that only the upper 3 coupons of Cluster 1 were relatively linear in corrosion rate.*

Discussion

From previous analyses, corrosion products (Table 2) have been determined on the coupons buried for 6, 12 and 18 months (Fell 2005) and 30 months (Fell, in prep). At six months, the corrosion products identified were principally iron oxyhydroxides and oxides – goethite, magnetite and maghemite. The presence of these oxidised species may in part be related to the presence of oxygen surrounding the samples at the time of burial, as well as a lower water table prior to the rewatering of the field at Fiskerton. However, analyses of the subsequent coupons, recovered at 12, 18 and 30 months, showed that the commonest corrosion products found on those from the lower waterlogged and partly waterlogged levels were siderite, and iron sulphides such as mackinawite, greigite and pyrite. Iron sulphides and siderite were also found on the archaeological iron artefacts recovered during excavations in 1981 and 2001 (Fell and Ward 1998; Fell and Williams 2004). Together, these results suggest that the lower coupons are largely anoxic, which is supported by the measurements of the groundwater levels and redox potentials (J. Williams pers comm). Usually associated with anoxic microbial reactions is the presence of hydrogen sulphide, which was very obviously present at the time that the rods of samples were extracted from the ground.

The primary corrosion products of anaerobic microbial corrosion are siderite and mackinawite (Tiller 1982, 139). Siderite confers stability to iron (Sontheimer et al 1981; Tiller 1982; Matthiesen et al 2003). It has been reported in mires, marine and other locations where it forms through the biological reduction of available iron oxides (eg Pye et al 1990), although it can form as scales in other, non-biological ways (Sontheimer et al 1981).

Siderite has occasionally been identified as a corrosion product at other sites, in particular on archaeological artefacts and on experimental coupons within anoxic waterlogged peatland at Nydam Mose, Denmark (Matthiesen et al 2003; Matthiesen et al 2004). Siderite, together with iron oxides, was identified on experimental iron in wet calcareous soils in laboratory tests (Angelini et al 1998). It has also been found on archaeological iron artefacts used as analogues within clay soils (Neff et al 2004).

From laboratory and field experiments, it is known that microbial corrosion is very aggressive unless protective films of corrosion products are formed (eg Smith and Miller 1975; Tiller 1982). These films can be protective under certain conditions, but if the film is broken, corrosion can be rapid. The occurrence of siderite requires a fairly neutral pH, low redox potential, low sulphide concentrations and high concentrations of carbonate (eg Matthiesen et al 2003, 190). The need for low levels of sulphide is due to the requirement that there is insufficient hydrogen sulphide (formed bacterially) to precipitate out the reduced iron as iron sulphide (eg Pye et al 1990), thus resulting in available ferrous ions. Carbonate and bicarbonate species are commonly formed during biogenic degradation of organic matter, although their origin may of course be geological.

Throughout the current project at Fiskerton, measurements of redox potential and pH have remained in the near neutral ranges. The water levels have become

more stable since rewatering in late 2004 although there are nevertheless fluctuations. This is supported by evidence of iron staining at Cluster 2 on the installation rods for the iron coupons (see Figure 1, centre) as well as stain rings on the installation tubes for the bone experiments (Figure 10).

Figure 10. Iron staining visible as rings around the tubing used for the bone burial experiments removed from Cluster 2 at 30 months. When in the ground, the tubes are proud of the soil surface by c. 0.2m which means that the widest iron staining ring (visible at the top of the right image) is c. 0.5m below ground level, and the lesser iron staining rings (visible below the widest ring) are deeper in the ground. Photos: Matthew Collins

The corrosion rates at Fiskerton range from 8 to 250 µm per year penetration at Cluster 1, and from 21 to 171 µm per year at Cluster 2. These severe corrosion rates are unexpected and difficult to explain given that the principal corrosion product identified is the non-aggressive siderite. The severest and most erratic corrosion occurred on the coupons that were close to or below the water table levels. Presumably, therefore, the sulphide layers that were formed were not protective, or had been disrupted and were then no longer protective. During study of the archaeological artefacts from the 1981 excavation, it was clear that the better preserved artefacts were those that were buried in the lowest levels of the site, well below the variations in water table.

For comparison, it is worth considering corrosion rates determined for other soils. Maximum general corrosion rates that are quoted for UK drained soils are in the range 35 to 50 µm per year (Shrier et al 1994, 3.19-3.20). However, local corrosion or pitting can be ten times as rapid, with UK tests giving a general maximum of 300µm per year (Shrier et al 1994, 3.19). Interestingly, although field tests in the US have generally indicated that corrosion rates reduce over time, apparently this has not always been the case in the UK where corrosion has often been proportional to burial duration (Shrier et al 1994, 3.20).

The above figures are for field tests for modern pipeline and other installations whereas the Fiskerton rates are more usefully compared with experimental iron within archaeological contexts, such as for example in the waterlogged peat at Nydam Mose, Denmark. Here, early results based on electrical impedance measurements gave rates of between 6 and 40 µm per year for coupons within the constantly waterlogged anoxic peat (Matthiesen et al 2003). Subsequent impedance readings show that the corrosion rates increase dramatically, to c. 130µm per year over two years of measurements. When determined by weight loss measurements, three coupons buried for less than two years averaged only 12µm per year (Matthiesen et al 2004). However, the authors consider that the electrical impedance method may give unreliably high results due to inherent practical problems, either with the probes or due to thick film formations at the coupons. They further comment that their experiments have not yet shown if the modern iron coupons will ever become stable or will continue to corrode.

Other results are available for iron coupons in well drained alkaline sandy soil at Xanten, Germany, where there is a mean corrosion rate of about 15 µm per year based on 500 days of exposure (Galliano et al 1998). In clay soils, archaeological artefacts serving as experimental analogues gave average rates of under 5µm per year (Neff et al 2004). All these results would seem to be closer to the general averages quoted earlier (Shrier et al 1994), although all are for relatively short periods of burial.

When the Fiskerton measurements are compared with the above results, this suggests that some considerable corrosion reactions have occurred at the water table level and below. Conceivably, therefore, the present water levels are insufficient to protect the clean surfaces of the modern experimental iron that has not had chance to develop well-formed corrosion layers. This need not necessarily matter for any archaeological iron artefacts surviving in the ground providing they have intact and protective corrosion layers. Nor do the results presented in this report deflect from the benefits of rewatering the site. However, there could be other contributing factors to the enhanced corrosion rates, such as changes in water chemistry (although to date the analytical evidence does not support this). Or the experimental procedure may be badly conceived (such as a poor method of preparing and attaching the coupons to the bars) although this does not allow for the low initial corrosion values that were gained, and were maintained on the uppermost coupons. On balance, the absence of protective films on the coupons, for whatever reason, seems to be the most plausible explanation for the aggressive corrosion.

Conclusions

The corrosion rates increase dramatically over the 30 month period of the study for all coupons except for the upper three coupons at Cluster 1, which are in drained, partly oxygenated soil. The corrosion products determined previously for the coupons lying near or below the water table are principally iron sulphides and siderite, which will have derived from anaerobic microbial activity. These constituents can be protective under certain conditions but if the protective

corrosion film is broken, microbial corrosion is otherwise very aggressive. The absence of protective films is the most likely reason for the aggressive corrosion on the experimental coupons at Fiskerton.

Acknowledgements

I thank Jim Williams for much assistance throughout the project and for supplying groundwater data, and Phil Good the tenant farmer for access to the land. The initial installations were made with advice and help from James Rackham and his auger, Ian Panter, Karla Graham, Roger Wilkes and Phil Wimbleton.

References

Angelini, E, Barberis, E, Bianco, P, Rosalbino, F and Ruatta, L 1998 'Effect of burial in different soils on the decay of iron artifacts: Laboratory investigation', in Mourey, W and Robbiola, L (eds) *Metal 98*, Proc ICOM Metals Conservation Group Conference, 27–29 May 1998, Draguignan, France, 106–110

Bardal, E 2004 *Corrosion and Protection,* London: Springer-Verlag

Brandes, E A (ed) 1983 *Smithells Metals Reference Book*, 6th edn. Butterworths

Fell, V 2005 'Fiskerton: Scientific Analysis of Corrosion Layers on Archaeological Iron Artefacts and from Experimental Iron Samples Buried for up to 18 months'. Centre for Archaeology Report 65/2005. Portsmouth: English Heritage

Fell, V, forthcoming. 'Iron', in Graham K et al (in prep), 'A woodland burial study: report on 6 month samples'. RDRS Report. Portsmouth: English Heritage

Fell, V, in preparation, 'Studying the effects of rewatering on the Iron Age causeway and artefacts'. Proceedings of a conference held at Lincoln, 24 June 2006. Witham Valley Archaeological Research Committee.

Fell, V, Graham, K, Simpson, P, Wilkes, R, Williams, J and Wimbleton, P 2005 'Equipment for the Installation of Experimental Materials at Fiskerton, Lincolnshire'. Centre for Archaeology Report 32/2005. Portsmouth: English Heritage

Fell, V and Ward, M 1998. 'Iron sulphides: Corrosion products on artifacts from waterlogged deposits', in Mourey, W and Robbiola, L (eds) *Metal 98*, Proc ICOM Metals Conservation Group Conference, 27–29 May 1998, Draguignan, France, 111–115

Fell, V and Williams, J, 2004 'Monitoring of archaeological and experimental iron at Fiskerton, England', in J Ashton and D Hallam (eds) *Metal 04*. Proceedings of the International Conference on Metals Conservation, Canberra, 4–8 October 2004. Canberra: National Museum of Australia, 17–27

Galliano, F, Gerwin, W and Menzel, K 1998 'Monitoring of metal corrosion and soil solution at two excavation sites and in the laboratory', in Mourey, W and Robbiola, L (eds) *Metal 98*, Proc ICOM Metals Conservation Group Conference, 27–29 May 1998, Draguignan, France, 87–91

Last, J 2005 *Archaeological prospection and monitoring at Fiskerton, Lincolnshire: a multi-stranded survey project.* Unpublished summary report compiled for English Heritage

Matthiesen, H, Hilbert, L R and Gregory, D J 2003 'Siderite as a Corrosion Product on Archaeological Iron from a Waterlogged Environment, *Studies in Conservation*, **48** (3), 183–194

Matthiesen, H, Hilbert, L R, Gregory, D and Sørensen, B 2004 'Long term corrosion of iron at the waterlogged site Nydam in Denmark: studies of environment, archaeological artefacts, and modern analogues, in: *Prediction of Long Term Corrosion Behaviour in Nuclear Waste Systems*. Proc International Workshop (Eurocorr 2004), Nice, 12–16 September 2004. ANDRA, 114–127

Neff, D, Dillmann, Ph, Vega, E and Reguer, S, 2004 'Long-term corrosion of archaeological iron artefacts'. Poster presented at 34th International Symposium on Archaeometry, 3–7 May 2004. Zaragoza, Spain

Pye, K, Dickson, J A D, Schiavon, N, Coleman, M L and Cox, M 1990 'Formation of siderite–Mg-calcite–iron sulphide concretions in intertidal marsh and sandflat sediments, north Norfolk, England', *Sedimentology **37**, 325*–343

Shrier, L L, Jarman, R A and Burtsein, G T (eds) 1994 *Corrosion* (3rd edn), *Vol 1 Metal/Environment Reactions, Vol 2 Corrosion Control*. Oxford: Butterworth-Heinemann

Smith, J S, and Miller, J D A 1975 'Nature of Sulphides and their Corrosive Effect on Ferrous Metals: A Review', *British Corrosion J* **10** (3) 136–143

Sontheimer, H, Kölle, W, and Snoeyink, V L 1981 'The siderite model of the formation of corrosion-resistant scales', *Journal American Water Works Association* **73** (11) 572–579

Thompson, D H 1971 'General Tests and Principles', in Ailor, W H (ed) *Handbook on Corrosion Testing and Evaluation*. Wiley and Sons, 155–141

Tiller, A K , 1982 'Aspects of Microbial Corrosion', in Parkins, R N (ed) *Corrosion Processes.* London: Applied science Publishers, 115–159

Wranglén, G 1985 *An Introduction to Corrosion and Protection of Metals.* London; Chapman and Hall

Williams, J 2005 'Groundwater monitoring', in Fell et al 2005, 6–10.

Appendix 1. Methods of calculating corrosion rate

The units employed for the calculations will depend on factors such as those used for measuring dimensions, and any desirability for whole units in the final results. If centimetres are used, units will not be SI units although where density (specific gravity) is involved, this is most conveniently expressed as $g.cm^{-3}$. The calculations are excruciating for the unwary and therefore some variations are demonstrated below. A variety of conversion factors can be applied between units (eg Shrier et al 1994, 21:62, table 21.27; Wranglén 1985, 238, table 16.2).

For example, to convert mass loss rate in grams per square metres per day ($g.m^{-2}.d^{-1}$) to millimetres per year penetration ($mm.y^{-1}$), multiply by 0.36525/density (ρ), where ρ is 7.87 g/cm^3 .

ie $\times 365.25 \times \frac{1}{\rho} \times 10^{-3}$ $(mm.y^{-1})$

Conversely, to convert from millimetres penetration per year ($mm.y^{-1}$) to grams per square metre per day ($gm^{-2}.d^{-1}$), multiply by 10^3/365.25 x density (ie x 2.74 x 7.87).

A. Calculations for mass loss method

The mass loss method of determining corrosion rate is the mass of metal turned into corrosion products per unit area of surface per unit of time. If expressed graphically, as *weight loss per unit area of surface* (y axis) by *time* (x axis), this provides a convenient way to see general trends. The full calculations for mass loss rate are as follows:

$$\text{Mass loss rate} = \frac{\text{weight loss}}{\text{surface area}} \times \frac{1}{\text{time}} \quad \text{..... (1a)}$$

$$\text{or} \quad \frac{W}{A} \times \frac{1}{T} \quad \text{..... (1b)}$$

Where W = mass loss
A = surface area
T = time

If dimensions are expressed in grams, millimetres and days, equation (1b) becomes:

$$\frac{W\ (g)}{A\ (mm^2)} \times \frac{1}{\text{days}} \quad (g.mm^{-2}.d^{-1}) \text{ ..... (1c)}$$

$$\text{or} \quad \frac{W\ (g)}{A\ (mm^2)} \times 10^6 \times \frac{1}{\text{days}} \quad (g.m^{-2}.d^{-1}) \text{ ..... (1d)}$$

$$\text{or} \quad \frac{W\ (g)}{A\ (m^2)} \times \frac{1}{\text{days}} \quad (g.m^{-2}.d^{-1}) \text{ ..... (1e)}$$

$$\text{or} \quad \frac{W\ (g)}{A\ (m^2)} \times \frac{1}{\text{days}} \times 365.25 \quad (g.m^{-2}.year^{-1}) \text{ ..... (1f)}$$

To convert mm^2 to cm^2, multiply by 10^{-2} ; To convert cm^2 to m^2, multiply by 10^{-4} ;
To convert mm^2 to m^2, multiply by 10^{-6}

B. Calculations for penetration rate method

The penetration rate is the increase in corrosion depth per unit time (or the increase in corrosion thickness per unit time). This can be converted from the mass loss equation shown above, or calculated from first principles. The method incorporates the density (**ρ**) of the uncorroded metal, which for ferritic metallic iron (99.9% Fe) is 7.87 $g.cm^{-3}$ (or 7.87 x 10^3 $kg.m^{-3}$), or a lesser density for a steel or where impurity levels are high (Brandes 1983, table 14.11).

B.1 To convert from mass loss rate

Mass loss rate $\frac{W\ (g)}{A\ (m^2)} \times \frac{1}{days}$ $(g.m^{-2}\ d^{-1})$ …….. (1e)

Penetration rate $= \frac{W\ (g)}{A\ (m^2)} \times \frac{1}{days} \times 365.25 \times \frac{1}{\rho} \times 10^{-3}$ $(mm.y^{-1})$ **……. (2)**

or $\frac{W\ (g)}{A\ (mm^2)} \times 10^6 \times \frac{1}{days} \times 365.25 \times \frac{1}{7.87} \times 10^{-3}$ $(mm.y^{-1})$ ……. (2a)

B.2 To calculate from first principles

Penetration rate can also be calculated from the following:

Penetration rate $= \frac{\text{volume of metal loss}}{\text{surface area}} \times \frac{1}{\text{time}}$ …….. (3)

Volume of metal loss = weight loss of metal / density $(g.cm^{-3})$ …….. (3a)

from $\rho = \frac{W}{V}$ $(g.cm^{-3})$

& $V = \frac{W}{\rho}$ (cm^3)

Where W = mass loss (g)
A = surface area (cm^2)
V = volume of corrosion products (cm^3)
ρ = density of iron at 20℃ is 7.87 $g.cm^{-3}$

Substituting into Equation (3) will give:

Penetration rate $= \frac{W}{\rho \times A \times T}$ **…… (3b)**

$$= \frac{W}{\rho \times A \times T} \quad (cm.y^{-1}) \quad \ldots\ldots\ldots\ldots\ldots\ldots \quad (3c)$$

If T = time in years

$$\text{or} \quad \frac{W}{\rho \times A \times T} \times 10 \quad (mm.y^{-1}) \quad \ldots\ldots\ldots\ldots\ldots\ldots \quad (3d)$$

$$\text{or} \quad \frac{W}{\rho \times A \times T} \times 10^{4} \quad (\mu m.y^{-1}) \quad \ldots\ldots\ldots\ldots\ldots\ldots \quad (3e)$$

The relevant burial durations for the Fiskerton coupons are as follows:

Nominal duration	**Burial duration**	**Real duration**		
		Days	**Weeks & days**	**Years**
6 month	22 Dec 2003 – 22 June 2004	183	26 wks	0.5010
12 month	22 Dec 2003 – 08 Dec 2004	351	50 wks 1 day	0.9610
18 month	22 Dec 2003 – 22 June 2005	547	78 wks 1 day	1.4986
30 month	22 Dec 2003 – 25 June 2006	915	130 wks 4 days	2.5051

One year is 365.25 days. 2004 was a leap year

For any set of samples, the value for duration and density can be abbreviated to ease the calculations. The density of the metallic iron (ρ) is a constant. From the burial durations in years, the factor 'ρ x T' in equations (3b) to (3e) above can be abbreviated as shown:

Nominal duration	ρ x T (years^{-1})
6 month	3.9460
12 month	7.5678
18 month	11.7939
30 month	19.7151

Appendix 2. Blanks used to test coupons in EDTA.Na_2 solution

a) Error tests made by submitting coupons from 12 month Cluster 2, Rod 1 to an additional 4 hours immersion in 5% EDTA.Na_2 solution. Weights shown in grams.

Coupon	Wt before	Wt after 4hr immersion in EDTA.Na_2	Wt loss 1	Wt after another 4 hr immersion in EDTA.Na_2	Wt loss 2	Error
1	4.63	4.17	0.46	4.17	0.46	0
2	4.46	3.99	0.47	3.99	0.47	0
3	5.92	5.57	0.35	5.57	0.35	0
4	4.23	3.82	0.41	3.82	0.41	0
5	2.42	1.96	0.46	1.96	0.46	0
6	3.55	3.14	0.41	3.14	0.41	0
7	5.15	4.84	0.31	4.84	0.31	0
8	5.01	4.86	0.15	4.85	0.16	0.01

b) Error tests made by submitting coupons 30 month Cluster 1, Rod 4 to an additional 24 hours immersion in 5% EDTA.Na_2 solution. Weights shown in grams.

Coupon	Wt before	Wt after 21 hr immersion in EDTA.Na_2	Wt loss 1	Wt after another 24 hr immersion in EDTA.Na_2	Wt loss 2	Error
1	8.54	3.19	5.35	3.14	5.4	0.05
2	6.82	4.17	2.65	4.12	2.7	0.05
3	7.38	3.05	4.33	3.02	4.36	0.03
4	5.87	0.79	5.08	0.77	0.79	0.02
5	5.75	0.85	4.90	0.85	0.85	0
6	4.35	3.98	0.37	3.87	0.48	0.11
7	7.59	7.25	0.34	7.15	0.44	0.10
8	8.51	8.21	0.30	8.13	0.38	0.08

c) Error tests made by submitting coupons 30 month Cluster 2, Rod 4 to an additional 24 hours immersion in 5% EDTA.Na_2 solution. Weights shown in grams.

Coupon	Wt before	Wt after 24 hr immersion in EDTA.Na_2	Wt loss 1	Wt after another 24 hr immersion in EDTA.Na_2	Wt loss 2	Error
1	7.87	4.90	2.97	4.84	3.03	0.06
2	7.97	6.19	1.78	6.10	1.88	0.09
3	7.09	4.09	3.00	3.95	3.14	0.14
4	6.36	3.83	2.53	3.78	2.58	0.05
5	7.11	3.13	3.98	3.11	4.00	0.02
6	8.54	5.61	2.93	5.59	2.95	0.02
7	7.93	6.26	1.67	6.23	1.70	0.03
8	6.25	5.39	0.86	5.35	0.90	0.04

Appendix 3. Dimensions* and weights of the iron coupons before burial

Coupon	Length (mm)	Width (mm)	Thickness (mm)	Weight (g)
Cluster 1. Rod 1				
1	48.3	7.7	2.2	5.75
2	52.1	7.8	1.8	5.51
3	48.9	8.9	2.2	6.52
4	49.0 (48.7-49.3)	8.7	2.1	6.35
5	49.7	8.2	2.0	6.26
6	53.7	8.3	2.2	6.86
7	50.5 (50.5-51.1)	8.3	2.3	6.39
8	52.7 (52.8-52.6)	7.3	1.8	4.46
Cluster 1. Rod 2				
1	49.3	7.6	2.1	5.89
2	51.7	8.9	2.0	6.81
3	50.8	8.1	2.0	5.95
4	49.5	7.7 (7.1-8.1)	2.5	6.65
5	52.8	9.1	2.1	7.18
6	49.1	7.8 (7.5-8.3)	2.3	6.43
7	52.7 (52.4-52.8)	7.7 (6.7-8.2)	1.1	4.14
8	52.2 (51.6-52.3)	8.9 (7.9-9.6)	1.9	6.48
Cluster 1. Rod 3				
1	51.0	7.7 (6.4-8.1)	1.7	5.38
2	50.0	6.8	2.4	5.88
3	50.1 (49.4-51.1)	8.4 (7.3-8.6)	1.9 (0.7-2.7)	5.62
4	52.2	6.8 (6.3-7.4)	1.9	5.22
5	51.8	7.1	1.7	4.41
6	52.8	6.8 (6.0-7.5)	1.9	5.19
7	51.6	7.1 (6.5-7.6)	1.9	5.18
8	52.5	7.2 (6.0-8.2)	1.7	4.88
Cluster 1. Rod 4				
1	56.4	10.5	1.9	8.54
2	50.9 (50.3-51.4)	8.0	2.4	6.82
3	51.4	8.4	1.9	7.38
4	50.5 (50.0-51.9)	7.6	2.3	5.87
5	51.9	8.1	1.8	5.75
6	50.9	8.5	1.2	4.35
7	54.5	10.0	1.7	7.59
8	51.1	9.9	2.8	8.51
Cluster 2. Rod 1				
1	52.3	6.7	1.8	4.63
2	49.3 (48.8-49.8)	6.6	1.6	4.46
3	50.03(?)	7.3	2.7	5.92
4	51.9	6.3 (5.1-7.8)	1.4	4.23
5	53.3	5.2	1.1	2.42

6	52.3	6.3	1.3	5.15
7	51.0	6.9	1.9	3.55
8	51.0	7.3	1.8	5.01
Cluster 2. Rod 2				
1	52.2	6.4 (5.7-7.4)	1.1	3.12
2	52.6 (52.7-53.8)	7.5	2.0	6.14
3	53.0	6.3	1.5	4.03
4	51.4 (51.3-51.5)	6.8	2.1	5.38
5	52.1	6.3 (5.3-6.8)	2.1	4.92
6	51.3	5.7	1.2	2.52
7	49.5 (49.0-50.2)	7.8	1.8 (1.1-2.8)	5.78
8	51.4	6.8 (5.2-7.8)	1.9	4.19
Cluster 2. Rod 3				
1	57.0	11.5	2.1	9.51
2	49.8	10.7	1.9	8.05
3	50.8	9.0	2.4	7.81
4	55.6	11.1	1.9	7.92
5	54.5 (54.0-55.3)	8.4	2.0	5.22
6	48.3	8.8 (7.5-9.6)	2.1	6.92
7	47.1 (46.9-47.5)	8.2 (6.8-9.1)	2.2	5.99
8	54.0 (53.0-54.3)	0.9	2.4	9.78
Cluster 2. Rod 4				
1	50.5 (49.6-51.0)	9.0	2.4	7.87
2	50.8	9.1	2.7	7.97
3	51.0 (50.5-51.5)	10.3	2.0	7.09
4	44.9 (44.4-45.4)	10.8	2.2	6.36
5	51.6 (50.6-52.2)	9.0	2.1	7.11
6	51.6 (51.3-52.2)	10.1	2.0	8.54
7	51.0 (50.6-51.4)	9.3	2.6	7.93
8	51.5 (50.6-52.4)	10.3 (8.0-11.4)	1.9	6.25

* Bracketed dimensions are the extremes; average dimensions given in brackets

Appendix 4. Calculations of surface area of the iron coupons before burial

Coupon	Length (mm)	Width (mm)	Thickness (mm)	Surface area mm^2	Surface area m^2
Cluster 1. Rod 1					
1	48.3	7.7	2.2	990.22	9.9022×10^{-4}
2	52.1	7.8	1.8	1028.40	10.2840×10^{-4}
3	48.9	8.9	2.2	1124.74	11.2474×10^{-4}
4	49.0	8.7	2.1	1094.94	10.9494×10^{-4}
5	49.7	8.2	2.0	1046.68	10.4668×10^{-4}
6	53.7	8.3	2.2	1164.22	11.6422×10^{-4}
7	50.5	8.3	2.3	1108.78	11.0878×10^{-4}
8	52.7	7.3	1.8	985.42	9.8542×10^{-4}
Cluster 1. Rod 2					
1	49.3	7.6	2.1	988.34	9.8834×10^{-4}
2	51.7	8.9	2.0	1162.66	11.6266×10^{-4}
3	50.8	8.1	2.0	1058.56	10.5856×10^{-4}
4	49.5	7.7	2.5	1048.30	10.4830×10^{-4}
5	52.8	9.1	2.1	1220.94	12.2094×10^{-4}
6	49.1	7.8	2.3	1027.70	10.2770×10^{-4}
7	52.7	7.7	2.0	1053.18	10.5318×10^{-4}
8	52.2	8.9	1.9	1161.34	11.6134×10^{-4}
Cluster 1. Rod 3					
1	51.0	7.7	1.7	984.98	9.8498×10^{-4}
2	50.0	6.8	2.4	952.64	9.5264×10^{-4}
3	50.1	8.4	1.9	1063.98	10.6398×10^{-4}
4	52.2	6.8	1.9	934.12	9.3412×10^{-4}
5	51.8	7.1	1.7	935.82	9.3582×10^{-4}
6	52.8	6.8	1.9	944.56	9.4456×10^{-4}
7	51.6	7.1	1.9	955.78	9.5578×10^{-4}
8	52.5	7.2	1.7	958.98	9.5598×10^{-4}
Cluster 1. Rod 4					
1	56.4	10.5	1.9	1438.62	14.3862×10^{-4}
2	50.9	8.0	2.4	1097.12	10.9712×10^{-4}
3	51.4	8.4	1.9	1090.76	10.9076×10^{-4}
4	50.5	7.6	2.3	1034.86	10.3486×10^{-4}
5	51.9	8.1	1.8	1056.78	10.5678×10^{-4}
6	50.9	8.5	1.2	1007.86	10.0786×10^{-4}
7	54.5	10.0	1.7	1309.30	13.0930×10^{-4}
8	51.1	9.9	2.8	1353.38	13.5338×10^{-4}
Cluster 2. Rod 1					
1	52.3	6.7	1.8	913.22	9.1322×10^{-4}
2	49.3	6.6	1.6	829.64	8.2964×10^{-4}
3	50.0	7.3	2.7	1040.02	10.4002×10^{-4}
4	51.9	6.3	1.4	816.90	8.1690×10^{-4}
5	53.3	5.2	1.1	683.02	6.8302×10^{-4}

6	52.3	6.3	1.3	811.34	8.1134×10^{-4}
7	51.0	6.9	1.9	923.82	9.2382×10^{-4}
8	51.0	7.3	1.8	954.48	9.5448×10^{-4}
Cluster 2. Rod 2					
1	52.2	6.4	1.1	797.08	7.9708×10^{-4}
2	52.6	7.5	2.0	1029.40	10.2940×10^{-4}
3	53.0	6.3	1.5	845.70	8.4570×10^{-4}
4	51.4	6.8	2.1	943.48	9.4348×10^{-4}
5	52.1	6.3	2.1	901.74	9.0174×10^{-4}
6	51.3	5.7	1.2	721.62	7.2162×10^{-4}
7	49.5	7.8	1.8	978.48	9.7848×10^{-4}
8	51.4	6.8	1.9	920.20	9.2020×10^{-4}
Cluster 2. Rod 3					
1	57.0	11.5	2.1	1598.70	15.9870×10^{-4}
2	49.8	10.7	1.9	1295.62	12.9562×10^{-4}
3	50.8	9.0	2.4	1201.44	12.0144×10^{-4}
4	55.6	11.1	1.9	1487.78	14.8778×10^{-4}
5	54.5	8.4	2.0	1155.42	11.5542×10^{-4}
6	48.3	8.8	2.1	1089.90	10.8990×10^{-4}
7	47.1	8.2	2.2	1015.76	10.1576×10^{-4}
8	54.0	0.9	2.4	1235.52	12.3552×10^{-4}
Cluster 2. Rod 4					
1	50.5	9.0	2.4	1194.60	11.9460×10^{-4}
2	50.8	9.1	2.7	1248.02	12.4802×10^{-4}
3	51.0	10.3	2.0	1295.80	12.9580×10^{-4}
4	44.9	10.8	2.2	1214.92	12.1492×10^{-4}
5	51.6	9.0	2.1	1183.32	11.8332×10^{-4}
6	51.6	10.1	2.0	1289.12	12.8912×10^{-4}
7	51.0	9.3	2.6	1262.16	12.6216×10^{-4}
8	51.5	10.3	1.9	1295.74	12.9574×10^{-4}

Appendix 5. Corrosion rate measurements for Cluster 1

Coupon	Weight (g)			Surface area m^2	Wt loss per unit area $g.m^{-2}$	Corrosion rate	
	Before burial	After burial	Mass loss			**Mass loss rate** $g.m^{-2}.d^{-1}$	**Penetration rate** $mm.y^{-1}x10^{-3}$ ($\mu m.yr^{-1}$)
6 months Cluster I Rod 1							
1	5.75	5.58	0.17	9.9022×10^{-4}	171	0.94	43
2	5.51	5.30	0.21	10.2840×10^{-4}	204	1.11	51
3	6.52	6.25	0.27	11.2474×10^{-4}	240	1.31	61
4	6.35	5.96	0.39	10.9494×10^{-4}	356	1.94	90
5	6.26	5.86	0.40	10.4668×10^{-4}	382	2.09	97
6	6.86	6.60	0.26	11.6422×10^{-4}	223	1.22	57
7	6.39	6.19	0.20	11.0878×10^{-4}	180	0.98	46
8	4.46	4.43	0.03	9.8542×10^{-4}	30	0.16	8
12 months Cluster 1 Rod 2							
1	5.89	5.65	0.24	9.8834×10^{-4}	242	0.69	32
2	6.81	6.05	0.76	11.6266×10^{-4}	653	1.86	86
3	5.95	5.59	0.36	10.5856×10^{-4}	340	0.97	45
4	6.65	5.88	0.77	10.4830×10^{-4}	734	2.09	97
5	7.18	6.46	0.72	12.2094×10^{-4}	589	1.68	78
6	6.43	6.05	0.38	10.2770×10^{-4}	369	1.05	49
7	4.14	3.92	0.22	10.5318×10^{-4}	209	0.59	28
8	6.48	6.33	0.15	11.6134×10^{-4}	129	0.37	17
18 months Cluster 1 Rod 3							
1	5.38	4.74	0.64	9.8498×10^{-4}	649	1.19	55
2	5.88	5.37	0.51	9.5264×10^{-4}	535	0.98	45
3	5.62	4.52	1.10	10.6398×10^{-4}	1034	1.89	88
4	5.22	4.20	1.02	9.3412×10^{-4}	1092	1.99	93
5	4.41	3.55	0.86	9.3582×10^{-4}	919	1.68	78
6	5.19	4.82	0.37	9.4456×10^{-4}	391	0.71	33
7	5.18	4.90	0.28	9.5578×10^{-4}	293	0.53	25
8	4.88	4.70	0.18	9.5898×10^{-4}	187	0.34	16
30 months Cluster 1 Rod 4							
1	8.54	3.14	5.40	14.3862×10^{-4}	3753	4.10	190
2	6.82	4.12	2.70	10.9712×10^{-4}	2461	2.69	125
3	7.38	3.02	4.36	10.9076×10^{-4}	3997	4.36	202
4	5.87	0.77	5.10	10.3486×10^{-4}	4928	5.38	250
5	5.75	0.85	4.90	10.5678×10^{-4}	4636	5.06	235
6	4.35	3.87	0.48	10.0786×10^{-4}	476	0.52	24
7	7.59	7.15	0.44	13.0930×10^{-4}	336	0.36	17
8	8.51	8.13	0.38	13.5338×10^{-4}	281	0.30	14

Appendix 6. Corrosion rate measurements for Cluster 2

Coupon	Weight (g)			Surface area m^2	Wt loss per unit area $g.m^{-2}$	Corrosion rate	
	Before burial	After burial	Mass loss			**Mass loss rate** $g.m^{-2}.d^{-1}$	**Penetration rate** $mm.y^{-1}x10^{-3}$ ($\mu m.yr^{-1}$)
6 months Cluster 2 Rod 2							
1	3.12	3.03	0.09	7.9708 $x10^{-4}$	113	0.62	28
2	6.14	5.97	0.17	10.2940 $x10^{-4}$	165	0.90	42
3	4.03	3.80	0.23	8.4570 $x10^{-4}$	272	1.48	69
4	5.38	5.18	0.20	9.4348 $x10^{-4}$	212	1.16	54
5	4.92	4.62	0.30	9.0174 $x10^{-4}$	332	1.82	84
6	2.52	2.26	0.26	7.2162 $x10^{-4}$	360	1.97	91
7	5.78	5.56	0.22	9.7848 $x10^{-4}$	225	1.23	57
8	4.19	3.90	0.29	9.2020 $x10^{-4}$	315	1.72	80
12 months Cluster 2 Rod 1							
1	4.63	4.17	0.46	9.1322 $x10^{-4}$	503	1.43	66
2	4.46	3.99	0.47	8.2964 $x10^{-4}$	566	1.61	75
3	5.92	5.57	0.35	10.4002 $x10^{-4}$	336	0.96	44
4	4.23	3.82	0.41	8.1690 $x10^{-4}$	502	1.43	66
5	2.42	1.96	0.46	6.8302 $x10^{-4}$	673	1.92	89
6	3.55	3.14	0.41	8.1134 $x10^{-4}$	505	1.44	67
7	5.15	4.84	0.31	9.2382 $x10^{-4}$	335	0.95	44
8	5.01	4.86	0.15	9.5448 $x10^{-4}$	157	0.45	21
18 months Cluster 2 Rod 3							
1	9.51	8.42	1.09	15.9870 $x10^{-4}$	681	1.24	58
2	8.05	7.09	0.96	12.9562 $x10^{-4}$	740	1.35	63
3	7.81	6.68	1.13	12.0144 $x10^{-4}$	940	1.72	80
4	7.92	7.00	0.92	14.8778 $x10^{-4}$	618	1.13	52
5	5.22	4.32	0.90	11.5542 $x10^{-4}$	779	1.42	66
6	6.92	6.06	0.86	10.8990 $x10^{-4}$	789	1.44	67
7	5.99	5.52	0.47	10.1576 $x10^{-4}$	462	0.85	39
8	9.78	9.47	0.31	12.3552 $x10^{-4}$	251	0.46	21
30 months Cluster 2 Rod 4							
1	7.87	4.84	3.03	11.9460 $x10^{-4}$	2536	2.77	128
2	7.97	6.10	1.88	12.4802 $x10^{-4}$	1506	1.64	76
3	7.09	3.95	3.14	12.9580 $x10^{-4}$	2423	2.65	123
4	6.36	3.78	2.58	12.1492 $x10^{-4}$	2123	2.32	107
5	7.11	3.11	4.00	11.8332 $x10^{-4}$	3380	3.69	171
6	8.54	5.59	2.95	12.8912 $x10^{-4}$	2288	2.50	116
7	7.93	6.23	1.70	12.6216 $x10^{-4}$	1347	1.47	68
8	6.25	5.35	0.90	12.9574 $x10^{-4}$	694	0.76	35